arXiv:1105.0504v3 [nucl-th] 17 May 2011

Theoretical study of the two-proton halo candidate ^{17}Ne including contributions from a resonant continuum and pairing correlations

Shi-Sheng Zhang,[1, 2, *] En-Guang Zhao,[2, 3] and Shan-Gui Zhou[2, 3]

[1] *School of Physics and Nuclear Energy Engineering,*
Beihang University, Beijing 100191, China
[2] *Institute of Theoretical Physics, Chinese Academy of Sciences, Beijing 100190, China*
[3] *Center of Theoretical Nuclear Physics,*
National Laboratory of Heavy Ion Accelerator, Lanzhou 730000, China

(Dated: January 20, 2013)

With the relativistic Coulomb wave function boundary condition, the energies, widths and wave functions of the single proton resonant states for ^{17}Ne are studied by the analytical continuation of the coupling constant (ACCC) approach within the framework of the relativistic mean field (RMF) theory. Pairing correlation and contribution from the single particle resonant states in the continuum are taken into good consideration by the resonant Bardeen-Cooper-Schrieffer (BCS) approach, in which constant pairing strength is used. It can be seen that the full self-consistent calculations with NL3 and NLSH effective interactions, agree well with the latest experimental measurements, such as binding energies, matter radii, charge radii and densities. The level of $\pi 2s_{1/2}$ states lies just above that of $\pi 1d_{5/2}$ and the occupation probability of the $(\pi 2s_{1/2})^2$ level is 20%, which are in accordance with the the shell model calculations.

Keywords: ^{17}Ne; single proton resonant states; binding energies; radii; densities; relativistic mean field model; analytical continuation of the coupling constant

PACS numbers: 21.60.-n Nuclear structure models and approaches, 21.10.-k, 24.10.Jv Relativistic models

---

[*] Electronic address: zss76@buaa.edu.cn

I. INTRODUCTION

The study of unbound or loosely bound exotic nuclei casts a new light on the discovery of nuclear halo structure [1]. The valence nucleons can be readily scattered into single-particle resonant states in the continuum. Due to the small binding energy and small or no centrifugal barrier conditions, the valence nucleons tunnel out of the potential barrier to long distances with an extended density tail to form the so-called halos. Therefore, the resonant states in the continuum and the coupling between bound states and the continuum near the threshold play an important role in the description of halo phenomena [2, 3]. In most calculations, the continuum is replaced by a set of positive energy states without the contribution of the widths, determined by solving the Hartree-Fock-Bogoliubov (HFB) or relativistic-Hartree-Bogoliubov (RHB) equations in coordinate space and with box boundary conditions [4, 5]. The properties of the quasipaticle resonant states in the continuum, such as the widths, are taken into account for the neutron case by the resonant Bardeen-Cooper-Schrieffer approach based on the relativistic mean field theory (RMF-rBCS) [6–8].

Neutron halos have been prominently observed in experiment [1, 9–12] and investigated for neutron rich nuclei theoretically [13–17], while those for proton halos are still few because of the Coulomb barrier [18–20], especially for the two-proton halo [21]. As one of the candidates, ^{17}Ne aroused great interest from both the experimental [22–24] and theoretical aspects [25–28]. Latest measurements of high-precision mass and charge radius on $^{17-22}$Ne, including the proton-halo candidate ^{17}Ne, have been performed with Penning trap mass spectrometry and collinear laser spectroscopy [23]. The charge radii of ^{17}Ne is determined for the first time, as well as the binding energy and root mean square (rms) experimental error bar. Recently, the reaction cross sections for ^{17}Ne are measured by transmission method and the corresponding density distribution is deduced from a modified Glauber-type calculation [24].

In the present paper, we focus on the properties of the single proton resonant states, which are extracted from the analytical continuation of the coupling constant (ACCC) approach within the framework of the RMF theory. A theoretical description of two-proton halo candidate ^{17}Ne is reasonably given, including the binding energy, matter radius, charge radius, density and occupation probabilities of the proton resonant states. The full self-consistent RMF+ACCC+BCS approach with the relativistic Coulomb wave functions boundary condition are used and systematically introduced in Sec. II. The numerical details are given in section III. We apply this scheme to calculate the proton resonant states in ^{17}Ne and compare the theoretical results and the experimental results. Finally, we give a brief summary in Sec. IV.

II. THEORETICAL FRAMEWORK

A. The Relativistic Mean Field Theory

The basic ansatz of the RMF theory is a Lagrangian density whereby nucleons are described as Dirac particles which interact via the exchange of various mesons (the scalar σ, vector ω and iso-vector vector ρ) and the photon [29–33]

$$\begin{aligned}\mathcal{L} &= \bar{\psi}(i\partial\!\!\!/ - M)\psi + \tfrac{1}{2}\partial_\mu\sigma\partial^\mu\sigma - U(\sigma) - \tfrac{1}{4}\Omega_{\mu\nu}\Omega^{\mu\nu} \\ &+\tfrac{1}{2}m_\omega^2\omega_\mu\omega^\mu - \tfrac{1}{4}\mathbf{R}_{\mu\nu}\mathbf{R}^{\mu\nu} + \tfrac{1}{2}m_\rho^2\boldsymbol{\rho}_\mu\boldsymbol{\rho}^\mu - \tfrac{1}{4}F_{\mu\nu}F^{\mu\nu} \\ &-g_\sigma\bar{\psi}\sigma\psi \;-\; g_\omega\bar{\psi}\omega\!\!\!/\psi \;-\; g_\rho\bar{\psi}\boldsymbol{\rho}\!\!\!/\boldsymbol{\tau}\psi - \; e\bar{\psi}\mathbf{A}\!\!\!/\psi,\end{aligned} \tag{1}$$

where M is the nucleon mass and m_σ (g_σ), m_ω (g_ω), and m_ρ (g_ρ) are the masses (coupling constants) of the respective mesons. A nonlinear scalar self-interaction $U(\sigma) = \dfrac{1}{2}m_\sigma^2\sigma^2 + \dfrac{g_2}{3}\sigma^3 + \dfrac{g_3}{4}\sigma^4$ of the σ meson has been included [34]. The field tensors for the vector mesons are given as

$$\begin{cases} \Omega^{\mu\nu} = \partial^\mu\omega^\nu - \partial^\nu\omega^\mu, \\ \mathbf{R}^{\mu\nu} = \partial^\mu\boldsymbol{\rho}^\nu - \partial^\nu\boldsymbol{\rho}^\mu - g^\rho(\boldsymbol{\rho}^\mu \times \boldsymbol{\rho}^\nu), \\ F^{\mu\nu} = \partial^\mu\mathbf{A}^\nu - \partial^\nu\mathbf{A}^\mu. \end{cases} \tag{2}$$

The classical variation principle gives the following equations of motion

$$[\boldsymbol{\alpha}\cdot\mathbf{p} + V_V(\mathbf{r}) + \beta(M + V_S(\mathbf{r}))]\psi_i \;=\; \epsilon_i\psi_i, \tag{3}$$

for the nucleon spinors, where ε_i and ψ_i are the single-particle energy and spinor wave function respectively, and the Klein-Gordon equations

$$\begin{cases} (-\Delta\sigma \ + \ U'(\sigma)) \ = \ g_\sigma \rho_s, \\ (-\Delta \ + \ m_\omega^2)\,\omega^\mu \ = \ g_\omega j^\mu(\mathbf{r}), \\ \left(-\Delta \ + \ m_\rho^2\right) \boldsymbol{\rho}^\mu \ = \ g_\rho \mathbf{j}^\mu(\mathbf{r}), \\ -\Delta \ A_0^\mu(\mathbf{r}) \ = \ e j_p^\mu(\mathbf{r}), \end{cases} \tag{4}$$

for the mesons, where

$$\begin{cases} V_V(\mathbf{r}) \ = \ g_\omega \omega^0 + g_\rho \tau_3 \rho_3^0 + \frac{1}{2} e(1-\tau_3)A^0, \\ V_S(\mathbf{r}) \ = \ g_\sigma \sigma, \end{cases} \tag{5}$$

are the vector and scalar potentials respectively and the source terms for the mesons are

$$\begin{cases} \rho_s \ = \ \sum\limits_{i=1}^{A} \bar{\psi}_i \psi_i, \\ j^\mu(\mathbf{r}) \ = \ \sum\limits_{i=1}^{A} \bar{\psi}_i \gamma^\mu \psi_i, \\ \mathbf{j}^\mu(\mathbf{r}) \ = \ \sum\limits_{i=1}^{A} \bar{\psi}_i \gamma^\mu \boldsymbol{\tau} \psi_i, \\ j_p^\mu(\mathbf{r}) \ = \ \sum\limits_{i=1}^{A} \bar{\psi}_i \gamma^\mu \frac{1-\tau_3}{2} \psi_i. \end{cases} \tag{6}$$

It should be noted that the contribution of negative energy states are neglected, i.e., the vacuum is not polarized. Moreover, the mean field approximation is carried out via replacing meson field operators in Eq. (3) by their expectation values, since the coupled equations Eq. (3) and Eq. (4) are nonlinear quantum field equations and their exact solutions are very complicated. In this way, the nucleons are assumed to move independently in the classical meson fields. The coupled equations can be solved self-consistently by iteration.

For spherical nuclei, the potential of the nucleon and the sources of meson fields depend only on the radial coordinate r. The spinor is characterized by the angular momentum quantum numbers l, j, m, the isospin $t = \pm\frac{1}{2}$ for the neutron and the proton respectively, and the other quantum number i. The Dirac spinor has the form

$$\psi(\mathbf{r}) = \begin{pmatrix} \mathrm{i} G_i^{lj}(r) Y_{jm}^l(\theta,\phi) \\ F_i^{lj}(r)(\boldsymbol{\sigma}\cdot\hat{\mathbf{r}}) Y_{jm}^l(\theta,\phi) \end{pmatrix} \frac{\chi_{\frac{1}{2}}(t)}{r}, \tag{7}$$

where $Y^l_{jm}(\theta,\phi)$ are the spinor spherical harmonics. The radial equation of the spinor, i.e. Eq. (3), can be reduced to [14]

$$\begin{aligned}\left(-\frac{\partial}{\partial r}+\frac{\kappa}{r}\right)F_i^{lj}(r)+\left[M+V_p(r)\right]G_i^{lj}(r) &= \varepsilon_i G_i^{lj}(r),\\ \left(\frac{\partial}{\partial r}+\frac{\kappa}{r}\right)G_i^{lj}(r)-\left[M-V_m(r)\right]F_i^{lj}(r) &= \varepsilon_i F_i^{lj}(r),\end{aligned} \tag{8}$$

in which $V_p(r)=V_V(r)+V_S(r)$, $V_m(r)=V_V(r)-V_S(r)$, and $\kappa=(-1)^{j+l+1/2}(j+1/2)$. The meson field equations can be reduced to

$$\left(\frac{\partial^2}{\partial r^2}-\frac{2}{r}\frac{\partial}{\partial r}+m_\phi^2\right)\phi=s_\phi(r), \tag{9}$$

where $\phi=\sigma$, ω, ρ, and photon ($m_\phi=0$ for photon). The source terms read

$$s_\phi(r)=\begin{cases}-g_\sigma\rho_s-g_2\sigma^2(r)-g_3\sigma^3(r) & \text{for the } \sigma \text{ field},\\ g_\omega\rho_v & \text{for the } \omega \text{ field},\\ g_\rho\rho_3(r) & \text{for the } \rho \text{ field},\\ e\rho_c(r) & \text{for the Coulomb field},\end{cases} \tag{10}$$

and

$$\begin{cases}4\pi r^2\rho_s(r) = \sum_{i=1}^{A}(|G_i(r)|^2-|F_i(r)|^2),\\ 4\pi r^2\rho_v(r) = \sum_{i=1}^{A}(|G_i(r)|^2+|F_i(r)|^2),\\ 4\pi r^2\rho_3(r) = \sum_{p=1}^{Z}(|G_p(r)|^2+|F_p(r)|^2)-\sum_{n=1}^{N}(|G_n(r)|^2+|F_n(r)|^2),\\ 4\pi r^2\rho_c(r) = \sum_{p=1}^{Z}(|G_p(r)|^2+|F_p(r)|^2).\end{cases} \tag{11}$$

By solving Eqs. (8) and (9) in a meshed box of size R_0 self-consistently, one can calculate the ground state properties of a nucleus. The vector potential $V_V(r)$ and the scalar potential $V_S(r)$, energies and wave functions for bound states are also obtained.

B. The RMF-ACCC approach

The ACCC approach as a bound-state-type method to study resonant states in the continuum, has the merit of numerical simplicity and easy to be implanted. The basic idea is a resonant state will become a bound state if one increases the attractive potential. Resonance parameters (i.e. energy and width) and wave function for a resonant state can be obtained by an analytic continuation from the bound-state solutions [35]. In our scheme, the continuation is carried out via a Padé approximant (PA).

It should be noted that the ACCC approach is applicable for the repulsive Coulomb case, which has been pointed out in Ref. [35]. In this sense, it can be used for proton decay because of the repulsive Coulomb potential. Within the framework of the nonrelativistic Schrödinger equation, the ACCC approach has been applied to study single-particle resonant states for proton decay in spherical and deformed nuclei in Woods-Saxon potentials [36].

By increasing the attractive potential as $V_p(r) \to \lambda V_p(r)$, a resonant state will be lowered and becomes a bound state if the coupling constant λ is large enough. Near the branch point λ_0, defined by the scattering threshold $k(\lambda_0) = 0$, the wave number $k(\lambda)$ behaves as

$$k(\lambda) \sim \begin{cases} i\sqrt{\lambda - \lambda_0}, & l > 0, \\ \\ i(\lambda - \lambda_0), & l = 0, \end{cases} \tag{12}$$

which is an ansatz in the relativistic framework inspired by Kukiulin [35] and confirmed to be good by our numerical calculation [37, 38]. These properties suggest an analytic continuation of the wave number k in the complex λ plane from the bound-state region into the resonance region by Padé approximant of the second kind (PAII) [35]

$$k(x) \approx k^{[L,N]}(x) = i\frac{c_0 + c_1 x + c_2 x^2 + \ldots + c_L x^L}{1 + d_1 x + d_2 x^2 + \ldots + d_N x^N}, \tag{13}$$

where $x \equiv \sqrt{\lambda - \lambda_0}$, and $c_0, c_1, \ldots, c_L, d_1, d_2, \ldots, d_N$ are the coefficients of PA. These coefficients can be determined by a set of reference points x_i and $k(x_i)$ obtained from the Dirac equation with $\lambda_i > \lambda_0,\ i = 1, 2, ..., L + N + 1$. With the complex wave number $k(\lambda = 1) = k_r + ik_i$, the resonance energy E and the width Γ can be extracted from the relation $\varepsilon = E - i\frac{\Gamma}{2}$ $(E, \Gamma \in \mathbb{R})$ and $k^2 = \varepsilon^2 - M^2$, i.e.,

$$\begin{aligned} E &= \sqrt{\left[\sqrt{(M^2 + k_r^2 - k_i^2)^2 + 4k_r^2 k_i^2} + (M^2 + k_r^2 - k_i^2)\right]/2} - M, \\ \Gamma &= \sqrt{2\sqrt{(M^2 + k_r^2 - k_i^2)^2 + 4k_r^2 k_i^2} - 2(M^2 + k_r^2 - k_i^2)}. \end{aligned} \tag{14}$$

In the non-relativistic limit ($k \ll M$), Eq. (14) reduces to

$$E = \frac{k_r^2 - k_i^2}{2M}, \qquad \Gamma = \frac{2k_r k_i}{M}. \tag{15}$$

It is evident that the continuation in the coupling constant can be replaced by the continuation in k plane along the $k(\lambda)$ trajectory determined by Eq. (13) to the point k_R corresponding to the wave number for Gamow state, i.e., $k_R = k^{[L,N]}(\lambda = 1)$ [35]. Similarly, the wave function $\varphi(k_R, r)$ for a resonant state can be obtained by an analytic continuation of the bound-state wave function $\varphi(k_i, r)$ in the complex k plane. One can also prove that the wave function $\varphi(k, r)$ is an analytic function of the wave number k in the inner region $r < R_0$ where the Jost function analyticity dominates [35]. Therefore, we use the technique, which has been adopted to find the complex resonance energy, to determine the resonance wave function $\varphi_R(r) = \varphi(k_R, r)$. Firstly, we construct the PA to define the resonance wave function at any point r in the inner region ($r < R_0$) [35]

$$\varphi^{[L',N']}(k,r) = \frac{P_{L'}(k,r)}{Q_{N'}(k,r)} = \frac{a_0(r) + a_1(r)k + a_2(r)k^2 + \ldots + a_{L'}(r)k^{L'}}{1 + b_1(r)k + b_2(r)k^2 + \ldots + b_{N'}(r)k^{N'}}, \tag{16}$$

where the coefficients $a_i(r)$ $(i = 0, 1, \ldots, L')$ and $b_j(r)$ $(j = 1, 2, \ldots, N')$ are dependent on r. These coefficients can be determined by a set of reference points k_i and $\varphi(k_i, r)$ obtained from the Dirac equation with $\lambda_i > \lambda_0$, $(i = 1, 2, ..., L'+N'+1)$. The resonance wave function $\varphi(k_R, r) = \varphi^{[L',N']}(k_R, r)$ $(r < R_0)$ can be extrapolated in this way. It should be noted that the resonance wave function can also be analytically continued by the bound-state wave function $\varphi(x_i, r)$ in the complex $x \equiv \sqrt{\lambda - \lambda_0}$ plane [35]. We also try to construct the PA to define the resonance wave function at any point r in the inner region ($r < R_0$) in the following way,

$$\varphi^{[L',N']}(x,r) = \frac{P_{L'}(x,r)}{Q_{N'}(x,r)} = \frac{a_0(r) + a_1(r)x + a_2(r)x^2 + \ldots + a_{L'}(r)x^{L'}}{1 + b_1(r)x + b_2(r)x^2 + \ldots + b_{N'}(r)x^{N'}}. \tag{17}$$

The variants in above expression have the same meaning as those in Eq. (16) except that the wave function k is replaced by x. Accordingly, the resonance wave function $\varphi_R(r) = \varphi^{[L',N']}(\sqrt{1-\lambda_0}, r)$ $(r < R_0)$ can be extrapolated in a similar way. Comparing the results of these two expressions Eq. (16) and Eq. (17), we found they are almost the same. In the following calculations, the wave function will be continued by Eq. (16), unless otherwise specified. The upper and lower components of the wave function in the inner part are both extracted from expression Eq. (16).

In the outer region ($r > R_0$, $V_{\text{nucl}}(r) \sim 0$), the asymptotic wave functions of the protons are the solutions of Eq. (8) in which $V_p(r) = V_m(r) = \dfrac{Z\alpha}{r}$, i.e.

$$\begin{aligned} \left(-\frac{\partial}{\partial r} + \frac{\kappa}{r}\right) F_i^{lj}(r) + \left[M - \frac{Z\alpha}{r}\right] G_i^{lj}(r) &= \varepsilon_i G_i^{lj}(r), \\ \left(\frac{\partial}{\partial r} + \frac{\kappa}{r}\right) G_i^{lj}(r) - \left[M - \frac{Z\alpha}{r}\right] F_i^{lj}(r) &= \varepsilon_i F_i^{lj}(r), \end{aligned} \tag{18}$$

in which α refers to fine structure constant and equals one in the natural unit ($\hbar = c = e = 1$). The final results for the upper and lower component are respectively [39],

$$G_\kappa^{\mathrm{R}}(kr) = \frac{\sqrt{\varepsilon_i + M}(2kr)^\gamma e^{-\pi y/2}|\Gamma(\gamma - iy)|}{2\sqrt{k\pi}\;\Gamma(2\gamma+1)} \{e^{-ikr+i\eta}(\gamma - iy)F(\gamma+1-iy, 2\gamma+1; 2ikr) + c.c.\}. \tag{19}$$

$$F_\kappa^{\mathrm{R}}(kr) = i\frac{\sqrt{\varepsilon_i - M}(2kr)^\gamma e^{-\pi y/2}|\Gamma(\gamma - iy)|}{2\sqrt{k\pi}\;\Gamma(2\gamma+1)} \{e^{-ikr+i\eta}(\gamma - iy)F(\gamma+1-iy, 2\gamma+1; 2ikr) - c.c.\}. \tag{20}$$

in which γ satisfied with $\gamma^2 = \kappa^2 - (Z\alpha)^2$, $y = \dfrac{Z\alpha\varepsilon_i}{k}$, $e^{2i\eta} = -\dfrac{\kappa + iyM/\varepsilon_i}{\gamma - iy}$, and the superscript R refers to the regular solutions of the wave function. Similarly, if γ is substituted by $-\gamma$, the irregular solutions of the wave function, $G_\kappa^{\mathrm{IR}}(kr)$ and $F_\kappa^{\mathrm{IR}}(kr)$ can be obtained in which IR refers to the irregular solutions.

The outer wave function is matched to the inner wave function at $r = r_m < R_0$

$$\varphi^{[L,N]}(k_R, r_m) = \frac{1}{C(k_R)}\left[G_\kappa^{\mathrm{R}}(k_R r_m) + D(k_R) G_\kappa^{\mathrm{IR}}(k_R r_m)\right], \tag{21}$$

where $C(k_R)$ and $D(k_R) = \tan\delta_\kappa(k_R)$ with $\delta_\kappa(k_R)$ the phase shift are the coefficients for matching. It has been found that $\delta_\kappa(k_R)$ is almost a constant when r_m is large enough. Given the upper component, the lower component $F_\kappa(r)$ can be calculated from the relationship between the upper and the lower components derived from Eq. (18), i.e.,

$$F_\kappa(k_R, r_m) = \frac{1}{C(k_R)}\left[F_\kappa^{\mathrm{R}}(k_R r_m) + D(k_R) F_\kappa^{\mathrm{IR}}(k_R r_m)\right], \tag{22}$$

Finally, the resonance wave function is normalized according to the Zel'dovich procedures [35].

C. The RMF+ACCC+BCS approach

On the basis of the RMF-ACCC approach, pairing correlation for open shell nuclei is treated by the BCS approximation with the width effect in resonant states of the continuum considered. That is so called the RMF+ACCC+BCS approach. The BCS approximation has the merit of simplicity, but thought to be not reliable for those nuclei near the drip line, due to the improper treatment of the continuous states [3, 40], i.e. the inclusion of the spurious continuous states which change with the box size. This can be solved by the proper treatment of resonant continuum in the pairing correlation, taking only the real resonant states into consideration and kicking the spurious continuous states off from the continuum [7, 8]. Therefore, the contribution of the continuum, especially for those single-particle resonant states in the continuum, to the pairing correlation for exotic nuclei is in great need of consideration.

The level density of the continuum [41] (single-particle resonant states)

$$g_\alpha(\varepsilon_\alpha) = \frac{1}{\pi}\frac{d\delta_\alpha}{d\varepsilon_\alpha} = \frac{1}{\pi}\frac{\Gamma/2}{(\varepsilon_r-\varepsilon_\alpha)^2+\Gamma^2/4} \ , \tag{23}$$

is introduced into the pairing gap equations instead of the discretized continuous states, in which δ_α is the phase shift of the scattering state with angular momentum (l_α, j_α), representing the variation of the localization of scattering states in the energy region of a resonance.

Suppose the pairing matrix elements are constant in the vicinity of the Fermi level [42], the gap equations can be rewritten as:

$$\sum_i \left(j_i+\frac{1}{2}\right)\frac{1}{\sqrt{(\varepsilon_i-\lambda)^2+\Delta^2}} + \sum_\alpha \left(j_\alpha+\frac{1}{2}\right)\int_{I_\alpha}\frac{g_\alpha(\varepsilon_\alpha)}{\sqrt{(\varepsilon_\alpha-\lambda)^2+\Delta^2}}d\varepsilon_\alpha = \frac{2}{G} \ , \tag{24}$$

$$\sum_i \left(j_i+\frac{1}{2}\right)\left[1-\frac{\varepsilon_i-\lambda}{\sqrt{(\varepsilon_i-\lambda)^2+\Delta^2}}\right] + \sum_\alpha \left(j_\alpha+\frac{1}{2}\right)\int_{I_\alpha} g_\alpha(\varepsilon_\alpha)\left[1-\frac{\varepsilon_\alpha-\lambda}{\sqrt{(\varepsilon_\alpha-\lambda)^2+\Delta^2}}\right]d\varepsilon_\alpha = N \ . \tag{25}$$

The sums i and α run over the bound states and resonant states involved in the pairing calculations, and I_α is an energy interval related to each partial wave (l_α, j_α). In this way, the contribution of the resonant states with width effect is naturally included. For a very narrow resonant state, the factor g_α becomes a delta function.

Taking account of those resonant continuum in the gap equations, the expressions of various densities should be modified as:

$$\begin{aligned} 4\pi r^2\rho_s(r) &= \sum_i (2j_i+1)v_i^2(|G_i(r)|^2-|F_i(r)|^2) \\ &\quad + \sum_\alpha (2j_\alpha+1)\int_{I_\alpha}(|G_\alpha(r)|^2-|F_\alpha(r)|^2)g_\alpha(\varepsilon_\alpha)v_\alpha^2(\varepsilon_\alpha)d\varepsilon_\alpha \ , \end{aligned} \tag{26}$$

$$\begin{aligned} 4\pi r^2\rho_v(r) &= \sum_i (2j_i+1)v_i^2(|G_i(r)|^2+|F_i(r)|^2) \\ &\quad + \sum_\alpha (2j_\alpha+1)\int_{I_\alpha}(|G_\alpha(r)|^2+|F_\alpha(r)|^2)g_\alpha(\varepsilon_\alpha)v_\alpha^2(\varepsilon_\alpha)d\varepsilon_\alpha \ , \end{aligned} \tag{27}$$

$$\begin{aligned} 4\pi r^2\rho_3(r) &= \sum_{p_i}(2j_{p_i}+1)v_{p_i}^2(|G_{p_i}(r)|^2+|F_{p_i}(r)|^2) \\ &\quad + \sum_{p_\alpha}(2j_{p_\alpha}+1)\int_{I_{p_\alpha}}(|G_{p_\alpha}(r)|^2+|F_{p_\alpha}(r)|^2)g_{p_\alpha}(\varepsilon_{p_\alpha})v_{p_\alpha}^2(\varepsilon_{p_\alpha})d\varepsilon_{p_\alpha} \\ &\quad - \sum_{n_i}(2j_{n_i}+1)v_{n_i}^2(|G_{n_i}(r)|^2+|F_{n_i}(r)|^2) \\ &\quad - \sum_{n_\alpha}(2j_{n_\alpha}+1)\int_{I_{n_\alpha}}(|G_{n_\alpha}(r)|^2+|F_{n_\alpha}(r)|^2)g_{n_\alpha}(\varepsilon_{n_\alpha})v_{n_\alpha}^2(\varepsilon_{n_\alpha})d\varepsilon_{n_\alpha} \ , \end{aligned} \tag{28}$$

$$\begin{aligned} 4\pi r^2\rho_c(r) &= \sum_{p_i}(2j_{p_i}+1)v_{p_i}^2(|G_{p_i}(r)|^2+|F_{p_i}(r)|^2) \\ &\quad + \sum_{p_\alpha}(2j_{p_\alpha}+1)\int_{I_{p_\alpha}}(|G_{p_\alpha}(r)|^2+|F_{p_\alpha}(r)|^2)g_{p_\alpha}(\varepsilon_{p_\alpha})v_{p_\alpha}^2(\varepsilon_{p_\alpha})d\varepsilon_{p_\alpha} \ . \end{aligned} \tag{29}$$

The Dirac equation, meson field functions as well as the photon field function with new densities Eqs. (26,27,28,29) are solved self-consistently in an iterative way. The total binding energy is given by the expression,

$$\begin{aligned} E &= E_{\text{nucleon}} + E_\sigma + E_\omega + E_\rho + E_c + E_{\text{pair}} + E_{\text{CM}} \\ &= \sum_i (2j_i+1)\, v_i^2 E_i + \sum_\alpha (2j_\alpha+1)\int_{I_\alpha} g_\alpha(\varepsilon_\alpha)v_\alpha^2(\varepsilon_\alpha)\varepsilon_\alpha d\varepsilon_\alpha \\ &\quad -\frac{1}{2}\int\left(g_\sigma\rho_s\sigma_0 + g_\omega\rho_\alpha\omega_0 + g_\rho\rho_3\rho_0^3 + e\rho_c A_0\right)d^3r - \int\left(\frac{1}{3}g_2\sigma_0^3 + \frac{1}{4}g_3\sigma_0^4\right)d^3r \\ &\quad -G\left[\sum_i\left(j_i+\frac{1}{2}\right)v_i u_i + \sum_\alpha\left(j_\alpha+\frac{1}{2}\right)\int_{I_\alpha} g_\alpha(\varepsilon_\alpha)v_\alpha(\varepsilon_\alpha)u_\alpha(\varepsilon_\alpha)d\varepsilon_\alpha\right]^2 \\ &\quad -\frac{3}{4}\cdot 41\cdot A^{-1/3} \ , \end{aligned} \tag{30}$$

in which the last two terms are the modified pairing energy and the correction for the spurious center of mass motion, respectively.

III. NUMERICAL DETAILS, RESULTS AND DISCUSSION

Using the single-particle energies and wave functions extracted from the RMF approach for bound states and the RMF-ACCC approach for resonant states with relativistic Coulomb wave functions boundary condition [43], we solve the BCS gap equations with the contribution of the continuum and obtain the Fermi energy, pairing gap as well as the occupation probabilities of quasi-particle states [8]. The nuclear densities composed of quasi-particle states are recalculated with the contribution of the widths. New meson field functions as well as the photon field function, and new potentials are used to recalculate the single-particle energies and wave functions of the bound states by solving coupled Dirac equations. New resonance parameters and wave functions are worked out by the RMF-ACCC approach. Therefore, the RMF+ACCC+BCS calculations are numerically self-consistent by an iterative way until convergency. In our calculations, the energies are in the precise of 10^{-3} MeV and that of the densities is 10^{-4} fm^{-3}.

It is our first attempt to describe the proton-rich odd nucleus in a fully self-consistent way by RMF+ACCC+BCS approach, with the consideration of the proton resonant continuum states contributions and pairing correlations. We are seriously eager to know how far we can go with our model. Furthermore, the recently improved experimental measurements for ^{17}Ne make it possible to give more possible comparison with our calculations. The pairing window is opened from all the bound states below the Fermi surface to one harmonic oscillator shell above the Fermi surface in our model, including the bound proton states $1s_{1/2}$, $1p_{3/2}$, $1p_{1/2}$, and single proton resonant states $1d_{5/2}$, $2s_{1/2}$. The constant pairing strength $G = C/A$ in the BCS approximation, is chosen by fitting the odd-even mass difference extracted from three-point formula,

$$\Delta_p = \frac{1}{2}[B(Z-1,N) - 2B(Z,N) + B(Z+1,N)], \tag{31}$$

in which the binding energies are taken from Ref. [44]. Highly excited resonant states with large widths, such as $1d_{3/2}$ and $1f_{7/2}$ are ignored in our calculations because of the minor occupation probability. For odd neutrons, the blocking effect is considered in the pairing correlation.

The theoretical binding energies for ^{17}Ne and ^{15}O are calculated by the RMF, RMF+BCS and RMF+ACCC+BCS approaches with NL3 and NLSH effective interactions [45, 46]. The results of the RMF+BCS approach change with the box size because of the inclusion of the spurious states. Therefore, only the binding energies obtained from the RMF and the RMF+ACCC+BCS approaches are shown in Tab. I. The available experimental binding energy for ^{17}Ne is 112.9276 MeV and that for ^{15}O is 111.955 MeV [44]. Asterisk denotes the result of the RMF+ACCC+BCS calculation without resonant width contribution. In this case, the resonant states with widths are regarded as the discrete positive states without widths. It can be seen from Tab. I that the results without width effect are larger than those with width contribution because of the over evaluation of the pairing correlation, which is also mentioned in Ref. [7]. The binding energies in the RMF+ACCC+BCS calculations are 1% larger than available data. Two-proton separation energy for ^{17}Ne is 0.97 MeV, and the corresponding theoretical one is about 0.03 MeV for NL3 and NLSH effective interactions. It should be noted that the binding energy for ^{15}O is larger than that for ^{17}Ne in the RMF calculations, which means ^{17}Ne is unstable against proton emission if pairing correlation is not taken into account. In the RMF+ACCC+BCS calculations, the binding energy for ^{15}O is less than that for ^{17}Ne, which means the valence protons are weakly bound in ^{17}Ne because of the attractive pairing correlation. As a consequence, pairing correlation is crucial in the existence of the nuclide and needs to be taken into good consideration. The contribution from the resonant state in the continuum to the pairing is as important as the bound states near the Fermi surface. The width of the resonant state has the effect of weakening the pairing gap and decreasing the binding energy. These factors are self-consistently included in our RMF+ACCC+BCS calculations so that the reasonable description of the binding energy can be given.

In order to show the contribution from the single particle energies to the whole binding energies, the single proton levels structure of ^{17}Ne are displayed in Tab. II, which are calculated by the full self-consistent RMF+ACCC+BCS approaches with NL3 and NLSH effective interactions, respectively. For protons, the bound states $1s_{1/2}$, $1p_{3/2}$, $1p_{1/2}$, as well as the single resonant states $1d_{5/2}$ and $2s_{1/2}$ with narrow widths, have quite similar structure for NL3 and NLSH effective interactions. The single proton levels in ^{17}Ne are plotted in Fig. 1 with NL3 effective interaction to show the levels positions for each resonant states in potential well and barrier. The proton potential with the Coulomb barrier V_p (red curve) corresponds to the potential for s partial wave and $V_p + l(l+1)/r^2$ (blue curve) refers to the proton potential with the Coulomb barrier and centrifugal barrier for d partial wave. It can be clearly seen that $2s_{1/2}$ state (red line) lies just below the Coulomb barrier ($l = 0$), and $1d_{5/2}$ (blue line) lies in the Coulomb and centrifugal barrier ($l = 2$). Therefore, s wave and d wave with positive energies lies just above the threshold and have the probabilities to tunnel the barrier, which are proportional to the widths of the single-particle states.

In Fig. 2, the density distributions in logarithm scale for the core nuclide ^{15}O and the two proton nuclide ^{17}Ne are presented with NL3 (solid line) and NLSH (dashed line) effective interactions, respectively. The error region for the experimental results are displayed by the gray area [24].

The radii of ^{15}O and ^{17}Ne are calculated by the RMF+ACCC+BCS approach. It can been seen that the densities from the RMF+ACCC+BCS approach agree well with the experimental fit results. The matter radius of ^{17}Ne increases if the proton pairing correlation effect is taken into account. The available experimental matter radius of ^{17}Ne is 2.75(7) fm and experimental charge radius is 3.042(21) fm. From the RMF+ACCC+BCS calculations, the rms radius of ^{17}Ne is about 2.86 fm for NL3 effective interaction, 2.78 fm for NLSH effective interaction; the charge radius of ^{17}Ne is about 3.15 fm for NL3 effective interaction, and 3.07 fm for NLSH effective interaction. We can conclude that the theoretical calculations agree well with the experimental measurements. The relative deviations are less than 5%.

In order to investigate the detailed contribution to the radii, we plot the occupation probabilities of the proton single-particle states $1\mathrm{s}_{1/2}$, $1\mathrm{p}_{3/2}$, $1\mathrm{p}_{1/2}$, $1\mathrm{d}_{5/2}$ and $2\mathrm{s}_{1/2}$ in ^{17}Ne by the RMF+ACCC+BCS approach in Fig. 3. In our calculations, the occupation probability of $(2\mathrm{s}_{1/2})^2$ is about 20%, and that for $(1\mathrm{d}_{5/2})^2$ is about 80% for the effective NL3 interaction, which is in accordance with the prediction in shell-model calculations [47, 48]. The real part of the wave functions for the upper component of proton resonant states $1\mathrm{d}_{5/2}$ and $2\mathrm{s}_{1/2}$ in ^{17}Ne by the RMF+ACCC+BCS approach are respectively plotted for NL3 and NLSH effective interactions in Fig. 4. The extension of the wave functions for $1\mathrm{d}_{5/2}$ and $2\mathrm{s}_{1/2}$ can be clearly seen at $r > 3$ fm, which give main contribution to the density of this range for ^{17}Ne.

Experimental studies [22–24, 49] still can not confirm the halo structure of ^{17}Ne. Corresponding theoretical studies are still controversial. Even if the binding energy, matter density and radius, agree with the experimental results, it is still hard to judge a halo nucleus because of small difference of the resonant levels. Therefore, the occupation probabilities of the resonant states $2\mathrm{s}_{1/2}$ and $1\mathrm{d}_{5/2}$ are discussed for the possibility of the halo existence. With a three-cluster model, Timofeyuk *et al.* obtain a $(2\mathrm{s}_{1/2})^2$-dominant configuration [50]. However a three-body model calculation by Garrido *et al.* suggested almost equal occupation probabilities of the $(2\mathrm{s}_{1/2})^2$ and $(1\mathrm{d}_{5/2})^2$ levels [51]. From the Coulomb mass shift, Nakamura *et al.* suggested a $(2\mathrm{s}_{1/2})^2$ dominance [52], but Fortune *et al.* oppositely suggested a $(1\mathrm{d}_{5/2})^2$ dominance [47]. By calculating the interaction cross sections σ_I with a Hartree-Fock type wave function and the Glauber model [53], Kitagawa *et al.* also proposed a $(1\mathrm{d}_{5/2})^2$ dominance. In our scheme, the occupation probability of $(1\mathrm{d}_{5/2})^2$ is larger than that of $(2\mathrm{s}_{1/2})^2$, because the single particle level for $\pi 2\mathrm{s}_{1/2}$ lies just above that for $\pi 1\mathrm{d}_{5/2}$.

For the neutron-rich nuclei close to the drip line, sd-shell structure may change so that the level $\nu 2\mathrm{s}_{1/2}$ and the level $\nu 1\mathrm{d}_{5/2}$ inverse, which leads to the magic number 16 [54]. For ^{17}Ne, if the inversion occurs, the occupation probability of $\pi 2\mathrm{s}_{1/2}$ will be enlarged to form halo. Meanwhile, the Coulomb barrier prevent the $\pi 2\mathrm{s}_{1/2}$ level falling. From this point of view, this new magic number 16 might not appear in proton-rich nuclei. At least, the inversion does not appear for ^{17}Ne in our present calculations. That means it is difficult to form halo. By taking some other effect into consideration, such as ρNN tensor coupling included in the RMF calculations [55], the inversion of the level $\nu 2\mathrm{s}_{1/2}$ and the level $\nu 1\mathrm{d}_{5/2}$ might occur. An effort on this point within the framework of RMF theory is in the process.

IV. SUMMARY

The energies, widths and wave functions of the single proton resonant states for ^{17}Ne are studied by RMF-ACCC approach with the relativistic Coulomb wave functions boundary condition. Pairing correlation and contribution from the single particle resonant states in the continuum are taken into good consideration by the resonant BCS approach, in which constant pairing strength are used. The full self-consistently microscopic RMF+ACCC+BCS calculations reproduce the experimental properties of two-proton halo candidate ^{17}Ne, such as the binding energies, matter radii, charge radii, densities with NL3 and NLSH effective interactions. The occupation probability of the proton resonant state $(\pi 2\mathrm{s}_{1/2})^2$ is in accordance with the prediction of the shell model. The resonant states in the continuum play an important role in the pairing correlation as well as those bound states near Fermi surface. The RMF+ACCC+BCS approach can take good consideration of the pairing correlation for proton-rich nuclei with only a few narrow resonant states and can be safely extrapolated to describe exotic nuclei. Since many nuclei are deformed, it is necessary to include the deformation effect in the model to describe the deformed exotic nuclei. We are developing the deformed RMF+ACCC+BCS approach to study the properties of the deformed nuclei.

Acknowledgments

This work was supported partially by the Fundamental Research Funds for the Central Universities, Key Laboratory of Micro-nano Measurement-Manipulation and Physics (Ministry of Education), the National Natural Science Foundation of China under Grant (No. 10875157, 10979066 and 10605004), Major State Basic Research Development Program of China (Grant No. 2007CB815000), Knowledge Innovation Project of Chinese Academy of Sciences (Grant Nos. KJCX2-EW-N01 and KJCX2-YW-N32). The authors express their gratitude to Prof. M. Fukuda for providing the data in Fig. 2. Helpful discussions with Prof. H. Sagawa, Prof. G. Colo, Prof. Zhongyu Ma, Prof. Yanlin Ye and Prof. I. Tanihata are gratefully acknowledged.

---

[1] I. Tanihata, H. Hamagaki, and O. Hashimoto *et al.*, Phys. Rev. Lett. **55**, 2676 (1985).

[2] A. Bulgac, FT-194-1980, CIP, Bucharest, see also arXiv:nucl-th/9907088.

[3] J. Dobaczewski, H. Flocard, and J. Treiner, Nucl. Phys. **A422**, 103 (1984).

[4] J. Dobaczewski, W. Nazarewicz, and T. R. Werner *et al.*, Phys. Rev. C **53**, 2809 (1996).

[5] J. Meng and P. Ring, Phys. Rev. Lett. **77**, 3963 (1996); J. Meng, Nucl. Phys. **A635**, 31 (1998).

[6] N. Sandulescu, L. S. Geng, H. Toki, and G. C. Hillhouse, Phys. Rev. C **68**, 054323 (2003).

[7] L. G. Cao and Z. Y. Ma, Eur. Phys. J. **A 22**, 189 (2004).

[8] S. S. Zhang, Int. J. Mod. Phys. **E 18**, 1761(2009).

[9] T. Aumann, A. Navin, D. P. Balamuth *et al.*, Phys. Rev. Lett. **84**, 35 (2000).

[10] Y. L. Ye, D. Y. Pang, G. L. Zhang *et al.*, J. Phys. **G 31**, S1647 (2005).

[11] P. Mueller, I. A. Sulai, A. C. C. Villari *et al.*, Phys. Rev. Lett. **99**, 252501 (2007).

[12] M. Smith, M. Brodeur, T. Brunner *et al.*, Phys. Rev. Lett. **101**, 202501 (2008).

[13] Z. Z. Ren, M. Mittig, B. Q. Chen *et al.*, Phys. Rev. C **52**, R1764 (1995).

[14] J. Meng, Nucl. Phys. **A635**, 31 (1998).

[15] J. Meng and P. Ring, Phys. Rev. Lett. **80**, 460 (1998). J. Meng, H. Toki, J. Y. Zeng, S. Q. Zhang, and S. G. Zhou, Phy. Rev. C **65**, 041302(R) (2002).

[16] Z. H. Liu, C. J. Lin, H. Q. Zhang *et al.*, Phys. Rev. C **64**, 034312 (2001).

[17] S. G. Zhou, J. Meng, P. Ring and E. G. Zhao, Phy. Rev. C **82**, 011301(R) (2010).

[18] Z. H. Liu, M. Ruan, Y. L. Zhao, H. Q. Zhang *et al.*, Phys. Rev. C **69**, 034326 (2004).

[19] F. Lu, H. Hua, Y. L. Ye *et al.*, Chin. Phys. C **33**, 170 (2009).

[20] Y. G. Ma, D. Q. Fang, C. W. Ma *et al.*, DYNAMICAL ASPECTS OF NUCLEAR FISSION, 191 (2008).

[21] Z. Z. Ren, B. Q. Chen, Z. Y. Ma and G. O. Xu, Phys. Rev. C **53**, R572 (1996).

[22] R. Kanungo, M. Chiba, S. Adhikari *et al.*, Phys. Lett. B **571**, 21 (2003).

[23] W. Geithner, T. Neff, and G. Audi *et al.*, Phys. Rev. Lett. **101**, 252502 (2008).

[24] K. Tanaka, M. Fukuda and M. Mihara *et al.*, Phys. Rev. C **82**, 044309 (2010).

[25] H. Y. Zhang, W. Q. Shen, Z. Z. Ren *et al.*, Chin. Phys. Lett. **20**, 1462 (2003).

[26] H. T. Fortune and R. Sherr, Phys. Lett. B **503**, 70 (2001).

[27] L. V. Grigorenko, Y. L. Parfenova and M. V. Zhukov, Phys. Rev. C **71**, 051604 (2005).

[28] Z. Y. Ma and Y. Tian, Sci. Chin. Seri. G (in press).

[29] B. D. Serot and J. D.Walecka, Adv. in Nucl. Phys. **16**, 1 (1986).

[30] P.-G. Reinhard, Rep. Prog. Phys. **52**, 439 (1989).

[31] P. Ring, Prog. Part. Nucl. Phys. **37**, 193 (1996).

[32] D. Vretenar, A. Afanasjev, G. A. Lalazissis *et al.*, Phys. Rep. **409**, 101 (2005).

[33] J. Meng, H. Toki, S. G. Zhou *et al.*, Prog. Part. Nucl. Phys, **57**, 470 (2006).

[34] J. Boguta and A. R. Bodmer, Nucl. Phys. **A292**, 413 (1977).

[35] V. I. Kukulin, V. M. Krasnopl'sky and J. Horácek, *Theory of Resonances: Principles and Applications* (Kluwer Academic, Dordrecht, 1989).

[36] G. Cattapan and E. Maglione, Phys. Rev. C **61**, 067301 (2000).

[37] N. Tanaka, Y. Suzuki, K. Varga, and R. G. Lovas, Phys. Rev. C **59**, 1391 (1999).

[38] S. C. Yang, J. Meng, and S. G. Zhou, Chin. Phys. Lett. **18**, 196 (2001).

[39] W. Greiner, *Relativistic Quantum Mechanics - Wave Equation* (Springer-Verlag, 1997).

[40] Junqing Li ,Zhongyu Ma, Baoqiu Chen, Yong Zhou, Phys. Rev. **C65**, 064305 (2002).

[41] P. Bonche, S. Levit, and D. Vautherin, Nucl. Phys. **A427**, 278 (1984).

[42] P. Ring and P. Schuck, "The Nuclear Many-Body Problem" (Springer-Verlag, Berlin, 1980).

[43] S. S. Zhang, W. Zhang, S. G. Zhou and J. Meng, Eur. Phys. J. A **32**, 43 (2007).

[44] A. H. Wapstra, G. Audi and C. Thibault, Nucl. Phys. **A729**, 129 (2003).

[45] G. A. Lalazissis, J.König and P.Ring, Phys. Rev. C **55**, 540 (1997).

[46] M. M. Sharma, M. A. Nagarajan, and P. Ring, Phys. Lett. **B 312**, 377 (1993).

[47] H. T. Fortune and R. Sherr, Phys. Lett. B **503**, 70 (2001); H. T. Fortune, R. Sherr and B. A. Brown, Phys. Rev. C **73**, 064310 (2006).

[48] N. Michel *et al.*, Nucl. Phys. **A703**, 202 (2002).

[49] R. Warner *et al.*, Nucl. Phys. **A635**, 292 (1998).

[50] N. K. Timofeyuk, P. Descouvemont, and D. Baye, Nucl. Phys. **A600**, 1 (1996).

[51] E. Garrido, D. V. Fedorov, and A. S. Jensen, Phys. Rev. C **69**, 024002 (2004); E. Garrido, D. V. Fedorov, and A. S. Jensen, Nucl. Phys. **A733**, 85 (2004).

[52] S. Nakamura, V. Guimaraes, and S. Kubono, Phys. Lett. B **416**, 1 (1998).

[53] H. Kitagawa, N. Tajima, and H. Sagawa, Z. Phys. A **358**, 381 (1997).

[54] A. Ozawa, T. Kobayashi, T. Suzuki, K. Yoshida, and I. Tanihata, Phys. Rev. Lett. **84**, 5493 (2000).

[55] W. Z. Jiang, Y. L. Zhao, Z. Y. Zhu and S. F. Shen, Phys. Rev. C **72**, 024313 (2005).

Tab. I: Binding energies of ^{17}Ne calculated by the RMF and the RMF+ACCC+BCS (this work) approach with NL3 and NLSH effective interactions, respectively, and compared with experimental binding energy ($B(^{17}\mathrm{Ne})$=112.928 MeV, $B(^{15}\mathrm{O})$=111.955 MeV) [44]. Two-proton separation energies $S_{2\mathrm{p}}$ are also shown for the RMF and the RMF+ACCC+BCS approach. All energy values are in unit of MeV. Asterisk denotes the result of the RMF+ACCC+BCS calculations without resonant width contribution.

	approach	$B_{\mathbf{NL3}}$	$B_{\mathbf{NL3}} - B_{\mathbf{Exp.}}$	$B_{\mathbf{NLSH}}$	$B_{\mathbf{NLSH}} - B_{\mathbf{Exp.}}$
^{17}Ne	RMF+ACCC+BCS	114.32	1.39	113.57	0.64
	RMF+ACCC+BCS*	114.84	1.91	114.11	1.18
	RMF	112.69	−0.24	111.86	−1.07
^{15}O	RMF+ACCC+BCS	114.30	2.77	113.54	2.72
	RMF	114.29	2.33	113.52	1.56
$S_{2\mathrm{p}}$	RMF+ACCC+BCS	0.02		0.03	
	RMF	−1.60		−1.66	

Tab. II: Single proton energy levels structure of ^{17}Ne with NL3 and NLSH effective interactions, respectively. All energy values are in unit of MeV.

πnl_j	NL3		NLSH	
	E	Γ	E	Γ
$2s_{1/2}$	0.74	0.02	1.17	0.18
$1d_{5/2}$	0.52	0.002	0.66	0.0026
$1p_{1/2}$	-8.94	0	-9.10	0
$1p_{3/2}$	-15.38	0	-15.79	0
$1s_{1/2}$	-35.46	0	-35.98	0

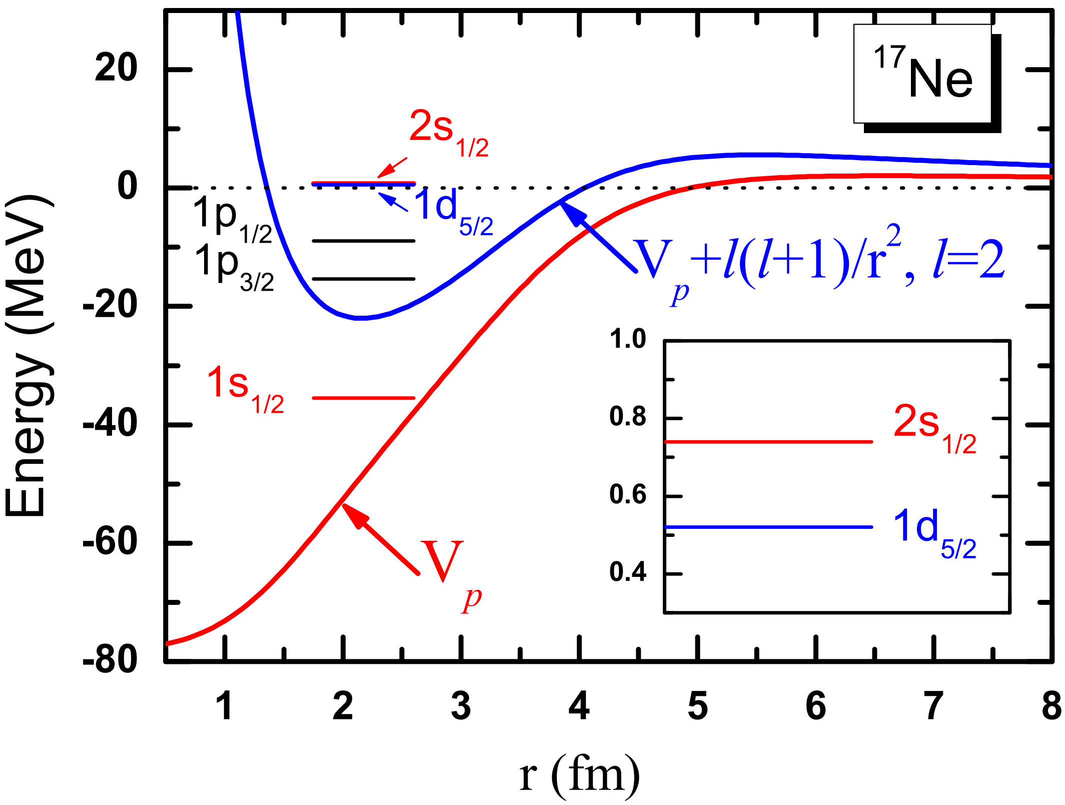

Fig. 1: (Color online) Single proton levels in ^{17}Ne calculated by the RMF+ACCC+BCS approach for effective interaction NL3.

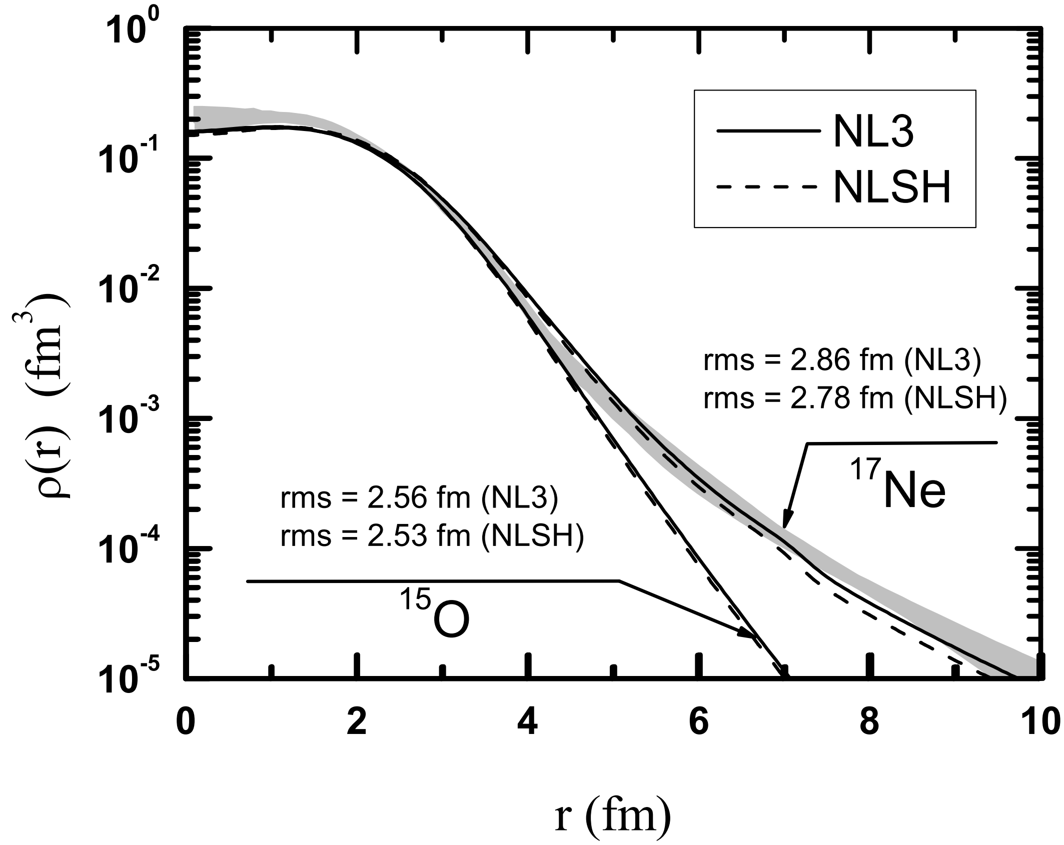

Fig. 2: Density distributions in logarithm scale for the core nuclide ^{15}O and ^{17}Ne in the RMF+ACCC+BCS calculations with NL3 (solid line) and NLSH (dashed line) effective interactions, respectively. The gray region corresponds to the error region for experimental results [24].

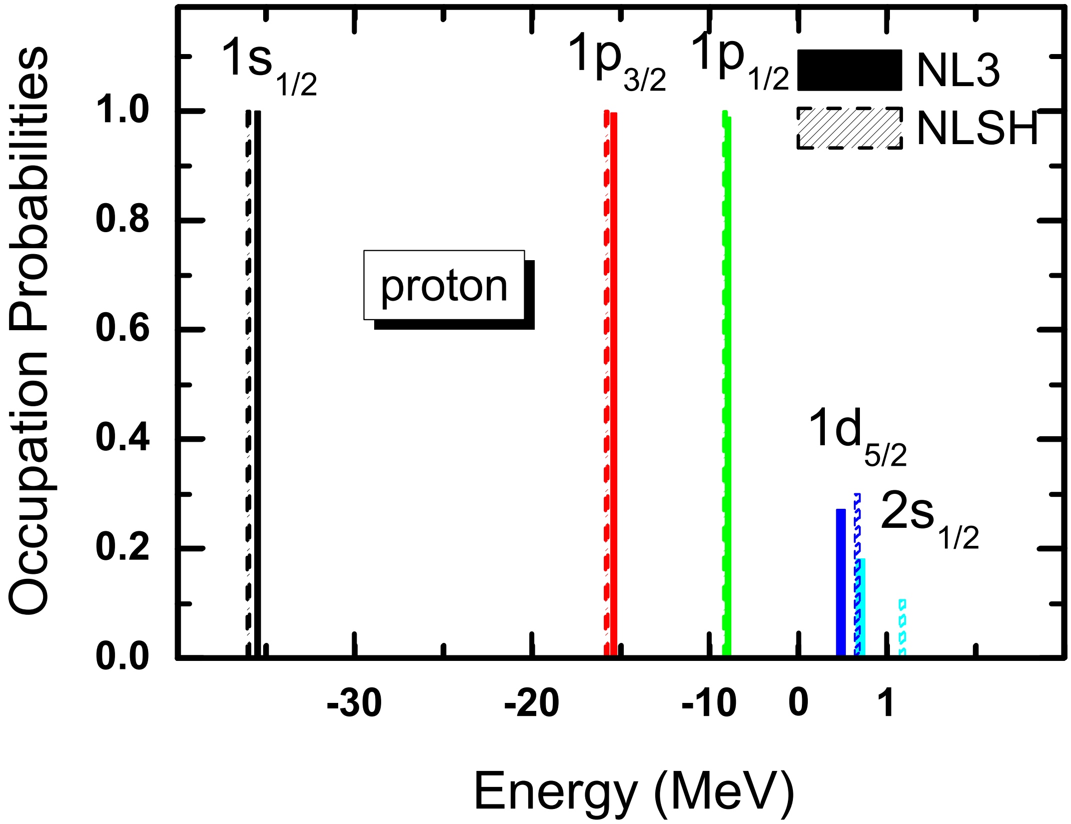

Fig. 3: (Color online) Occupation probabilities of the proton single-particle states $1s_{1/2}$, $1p_{3/2}$, $1p_{1/2}$, $1d_{5/2}$ and $2s_{1/2}$ in ^{17}Ne by the RMF+ACCC+BCS approach.

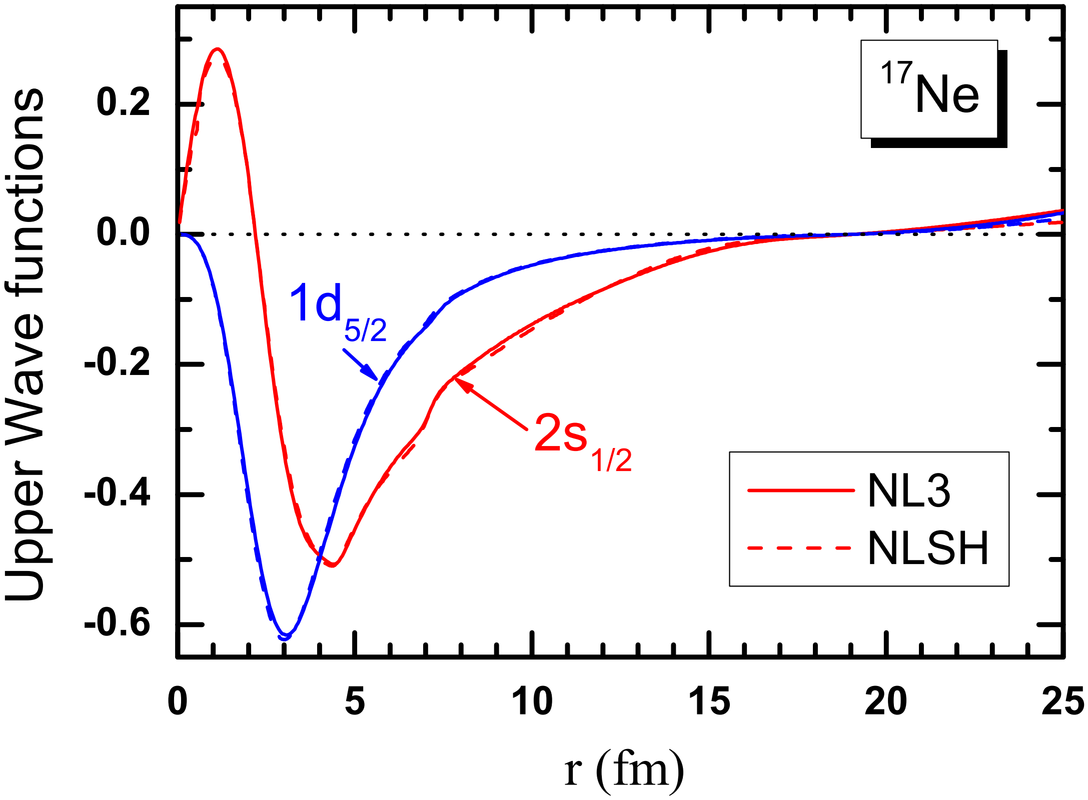

Fig. 4: (Color online) Upper wave functions for proton resonant states 1d$_{5/2}$ and 2s$_{1/2}$ in ^{17}Ne by the RMF+ACCC+BCS approach.